

Three-dimensional transient numerical simulation for intake process in the engine intake port-valve-cylinder system

LUO Ma-ji(罗马吉)[†], CHEN Guo-hua(陈国华), MA Yuan-hao(马元镐)

(*College of Energy and Power Engineering, Huazhong University of Science and Technology, Wuhan 430074, China*)

[†]E-mail: zanelmj@21.cn.com

Received Aug. 8, 2002; revision accepted Dec. 10, 2002

Abstract: This paper presents a KIVA-3 code based numerical model for three-dimensional transient intake flow in the intake port-valve-cylinder system of internal combustion engine using body-fitted technique, which can be used in numerical study on internal combustion engine with vertical and inclined valves, and has higher calculation precision. A numerical simulation (on the intake process of a two-valve engine with a semi-sphere combustion chamber and a radial intake port) is provided for analysis of the velocity field and pressure field of different plane at different crank angles. The results revealed the formation of the tumble motion, the evolution of flow field parameters and the variation of tumble ratios as important information for the design of engine intake system.

Key Words: Internal combustion engine, Intake flow, Transient numerical simulation, Dynamic grid generation

Document code: A

CLC Number: TK411.3

INTRODUCTION

The internal combustion engine is the most widely used power machinery in modern society, but is also one of the biggest environmental pollutant sources. To meet more and more stringent emission requirements, many advanced techniques, such as the lean burn technique, multi-valve technique and tumble technique, are adopted in gasoline engines (Iwamoto *et al.*, 1997; Kaoru *et al.*, 1992; Shi, 2001). These techniques are closely related with the in-cylinder gas flow motion generated during the intake process. For example, in gasoline direct injection engines, special intake ports are used by the tumble technique to organize in-cylinder large-scale gas rotation, whose rotation (tumble motion) axis is vertical to the cylinder axis. Tumble motion can promote fuel atomization, evaporation and mixing. Deep and detailed research on the in-cylinder gas flow produced during the intake process is helpful for achieving efficient control and utilization of the in-cylinder flow in the development and improvement of engine designs to improve combustion, enhance performance and reduce emissions.

There are two approaches for investigating

the in-cylinder flows: laser diagnostic measurement (Reeves *et al.*, 1999; Reuss *et al.*, 1989) and three-dimensional numerical simulation. The former is usually costly and time consuming and has limitations in the measurable parameters. With the development of computer techniques and computational fluid dynamics (CFD), 3D numerical simulation approach is widely used in the investigation of intake flow. This approach can yield detailed flow information and does not have the limitations mentioned above.

Transient numerical simulation of the intake flow is a challenging task because of the complicated geometry with a piston and one or multiple moving valves. The KIVA-3 code (Amsden, 1993) developed at Los Alamos National Laboratory has been widely used in multi-dimensional numerical simulation of the flow, combustion and emission in internal combustion engines. But it cannot deal with the moving valve. In order to conduct 3D transient numerical simulation for intake process using KIVA-3 code, the snapper technique was used to treat the moving vertical valves of diesel engines by Hessel (1993), in which the valves' axes are parallel to the cylinder axis. However, valves in gasoline engines are almost inclined. Kim *et al.* (2000) adopted

the obstacle cell model to treat the valve. This method reduces the difficulty of computational grid generation because no valves are considered in constructing the computational grid. But larger error was brought to the calculation results by the coarse fitting to the valve shape. In order to conduct 3D transient numerical simulation of intake flow in the intake port-valve-cylinder system of a high-speed small gasoline engine, a body-fitted valve model is added to KIVA-3 code. The valve model put forward in this paper can treat vertical and inclined valves, and has higher calculation precision.

NUMERICAL ANALYTIC MODEL

1. Numerical methods

The governing equations of gas flow consist of the mass, momentum and energy conservation equations, k - ϵ turbulence equations, equations of gas state relation and other auxiliary relations. For details, see Amsden *et al.* (1989) and Luo *et al.* (2001).

The governing equations are discretized by the arbitrary Lagrangian-Eulerian (ALE) method (Hirt *et al.*, 1974) for structured non-orthogonal meshes. The scalar quantities including the pressure are defined at the cell centers, while the velocity vectors are defined at the corner vertices of each cell. A transient solution to the discretized governing equations is given in a sequence of time steps or cycles. At each cycle the values of the dependent variables are calculated from those at the previous cycle. In the ALE

method, each cycle is divided into two fractional steps, the Lagrangian step and the rezone step. In the Lagrangian step the vertices move with the fluid velocity with no convection occurring across cell boundaries. In the rezone step the flow field is frozen as the vertices are moved to new user-specified positions. The flow field is rezoned onto the new computational mesh by convecting material across the boundaries of the computational cells. The Lagrangian step is again divided into phase A and phase B. The source terms are calculated in phase A. The pressure gradient and diffusion terms are calculated implicitly in phase B. In the rezone step, or phase C, all the convective terms are calculated explicitly by subcycling with submultiples of the main time step to satisfy the Courant condition.

2. Body-fitted valve model

To exactly fit the valve shape, the body-fitted technique is used to establish the valve model. In the body-fitted valve model, the shape of the valve (including the valve stem) is represented by surface body-fitted grid in the grid generation, and vertices on the surface body-fitted grids move according to the valve moving schedules in the flow calculation. The valve moving schedules include the intake valve lift profile and the intake valve moving velocity profile, as shown in Fig. 1a and 1b. Considering the stability of the numerical simulation, it is assumed that there exists a minimum valve lift from intake valve closure to opening, then the intake valve moves according to the valve moving schedules.

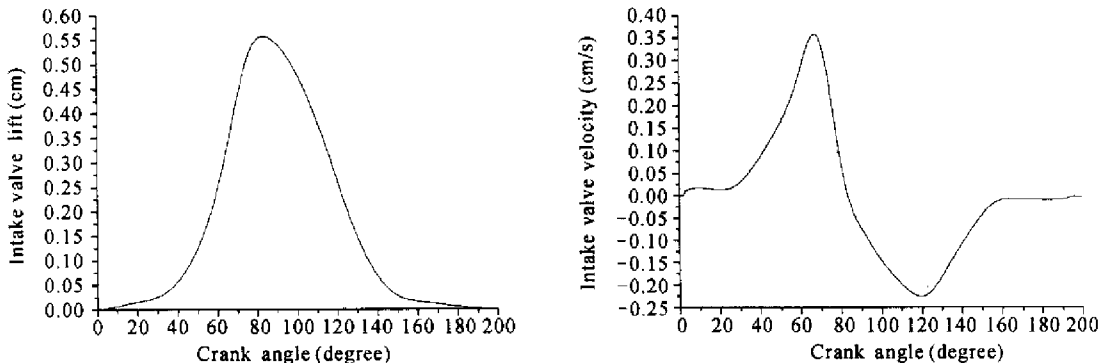


Fig.1 Intake valve moving schedules

(a) intake valve lift profile; (b) intake valve velocity profile

3. Geometry and grid generation

The geometry used in this study is the exact geometry of the intake port-valve-cylinder system in a high-speed small motorcycle engine. The engine specifications are summarized in Table 1. Fig. 2 is the 3D model of the computational domain. Because of the semi-spherical combustion chamber and the inclined intake valve, it is difficult to generate the 3D body-fitted grid for the computational domain, including the initial computational grid generation and dynamic grid generation.

Table 1 Engine specifications of the motorcycle engine

Bore	50.0 mm
Stroke	49.5 mm
Speed	4500 r/min
Compression ratio	9.1
Displacement volume	997 cm ³
Intake valve opening	0° CA after TDC
Intake valve closure	20° CA after BDC
Exhaust valve opening	30° CA before BDC
Exhaust valve closure	2.5° CA before TDC

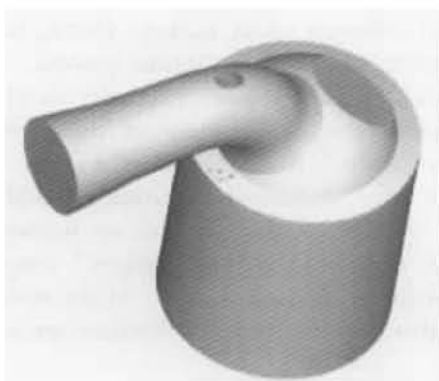


Fig. 2 3D geometry of computational domain

Initial grid generation is one of the key techniques in 3D transient simulation of the intake process. The block-structured grid generation method (Luo *et al.*, 2000) is adopted to generate the 3D body-fitted grid of the computational domain, as shown in Fig. 3. In the block-structured grid generation method, the complex computational domain is divided into many blocks according to the blocking rule first, then the elliptic grid generation approach is used to gener-

ate 3D body-fitted grid for each block, and finally the block grids are patched together by patching technique to generate the 3D integrated computational grid.

Dynamic grid generation is another key technique in 3D transient simulation of the intake process. Due to the piston and valve movement, the computational domain varies continuously as a function of crank angle. In order to dynamically adopt the computational grids to the variation of the computational domain, the computational grids are rezoned at different positions of the piston and valve. The snapper technique is used to maintain a reasonable axial mesh size as the piston moves between the top dead center (TDC) and the bottom dead center (BDC). When the piston moves up and the prerequisite is satisfied, planes are deactivated. On the contrary, when the piston moves down and the prerequisite is satisfied, ghost planes are activated. During the whole simulation, the lowest plane coincides with the piston crown and moves at the piston speed in a Lagrangian fashion. The dynamic grids induced by the valve movement are generated by the grid re-meshing method, the basic idea of which is to regenerate the local grids near the valve at each time step (corresponding to each new valve position). The re-meshing grids are generated by the elliptic grid generation approach.

4. Initial and boundary conditions

The calculation is carried out throughout the intake process, starting at the intake valve opening (IVO, at 0° ATDC, after top dead center) and ending at the intake valve closure (IVC, at 200° ATDC). Initially, gas in the cylinder is assumed to be quiescent at the measured pressure (1.1491×10^5 Pa) and temperature (360.0 K). Gas in the intake port is assumed to be quiescent at the intake pressure (0.85×10^5 Pa) and intake temperature (300.0 K) obtained from the engine quasi-dimensional cycle simulation. The boundary conditions at the intake port inlet are specified as the intake pressure and intake temperature.

On wall boundaries, law-of-the-wall boundary layer condition is imposed for the velocity. The fixed wall temperature condition is imposed for temperature.

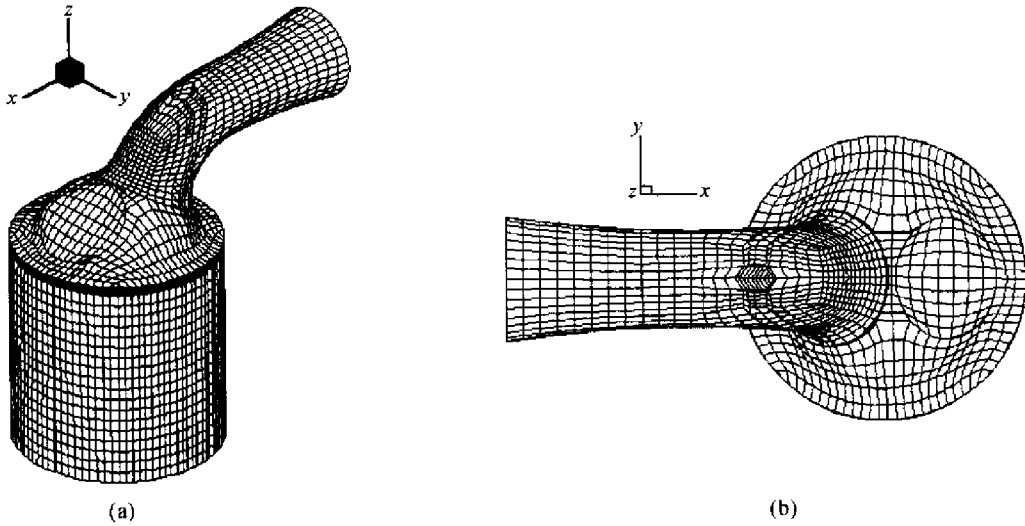


Fig.3 Computational grids of the intake port-valve-cylinder system
(a) perspective view; (b) top view

CALCULATION RESULTS AND DISCUSSIONS

1. Velocity fields

Two sectional planes are defined to investigate the flow field in the cylinder. One is the symmetric plane of the port and the cylinder (xz plane). The other is the plane that passes through the cylinder axis and is vertical to the xz plane (yz plane).

The velocity fields on the xz -plane are shown at different crank angles in Fig.4. As the intake valve start to open, there is some backflow into the intake port due to the higher gas pressure in the cylinder over the intake port pressure. At 25 degree crank angle (25° CA) the jet-like intake flow develops into a pair of counter-rotating small vortices under the intake valve, that is the dual-vortex structure. As the piston moves towards bottom dead center (BDC), the dual-vortex structure is more evident and the vortex on the side of intake valve is stronger than that on the side of exhaust valve. After 120° CA, the vortex at the side of the intake valve becomes weaker and the other vortex becomes stronger. By the end of the intake process, the vortex on the exhaust side develops into a large scale tumbling motion that dominates the flow structure in the xz -plane.

The flow field evolution on the xz -plane indicates that the in-cylinder tumble motion is formed

at the late stage of the intake process; and that the in-cylinder flow structure set up during the intake process is mainly affected by the flow toward the exhaust side. If the flow is strengthened, the in-cylinder tumble motion will be stronger.

Fig.5 shows the velocity fields on the yz -plane at different crank angles. During the early and middle stages of the intake process, two intake flow jets form a pair of counter-rotating vortices under the confinement of the combustion chamber walls. Around 150° CA, the pair of vortices have weakened to disappear and a new pair of counter-rotating vortices are formed at the cylinder center. The new vortices' cores move down with the moving piston. At the time of intake valve closure, the new vortices are still evident.

2. Pressure fields

The pressure distributions on the xz -plane are shown in Fig.6. They indicate the behaviors of flow resistance during the intake process are different. At the beginning of intake valve opening, the in-cylinder pressure is higher than that in the port, so gas in the cylinder flows back towards the intake port. During the early intake process (from 20° CA to 60° CA), due to the low valve lift (2.52 mm at 60° CA), the intake pressure drop of the port-valve-cylinder system mainly concentrates near the intake valve. The intake pressure loss is principally caused by the

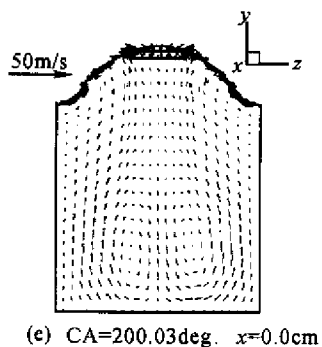
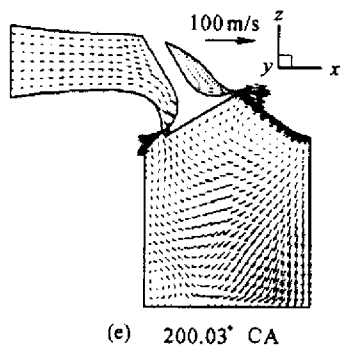
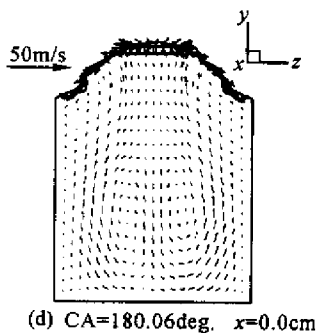
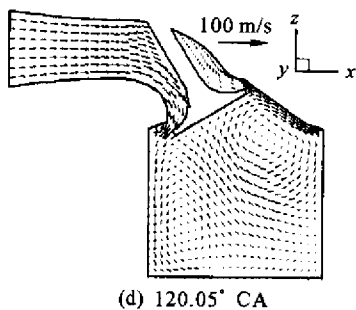
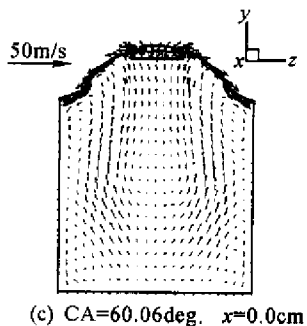
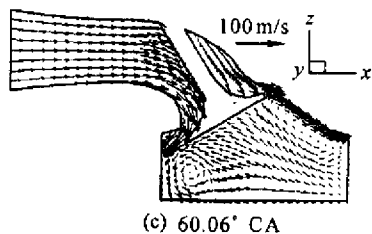
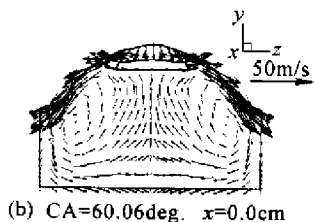
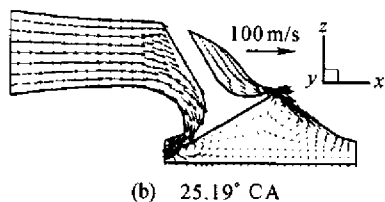
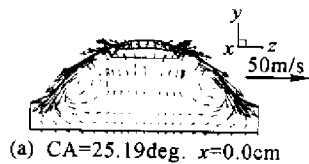
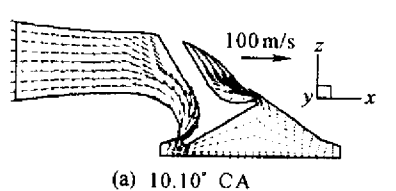


Fig.4 Velocity fields on the xz-plane

Fig.5 Velocity fields on the yz-plane

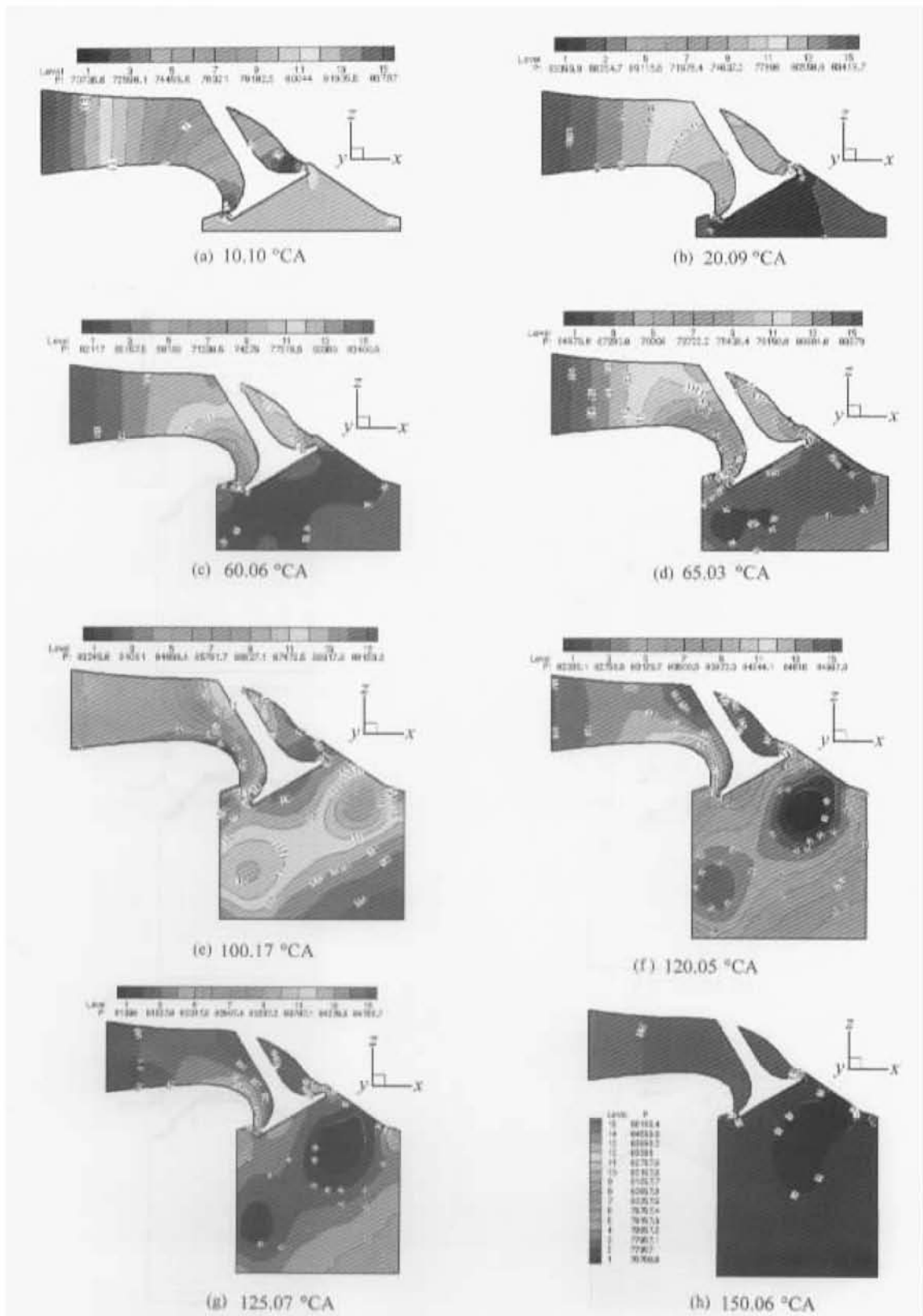


Fig.6 Pressure fields on the xz-plane

valve's obstruction. During the middle intake process (from 60° CA to 120° CA), the intake lift becomes higher and the loss is dominated by the resistance of the intake port, rather than by the valve's obstruction. The valve lift decreases during the late intake process. When the valve gap is small enough, the major intake resistance changes from the resistance of the intake port curved section to that of the valve gap. The transitional point is near 120° CA when the valve lift is about 2.5 mm. At 150° CA, the valve lift is very small and the pressure in the port and the cylinder are almost uniform at different pressure values. From Fig. 6 it also can be seen that the pressure distributions in the cylinder are uneven during the intake process.

3. Integrated flow parameters

To characterize the in-cylinder large-scale flow structure, tumble ratios R_{ty} and R_{tx} are defined as (Kim *et al.*, 2000):

$$R_{ty} = \frac{60H_y}{2\pi M_y \omega} \quad (1)$$

$$R_{tx} = \frac{60H_x}{2\pi M_x \omega} \quad (2)$$

where H_y is the angular momentum of the in-cylinder gas about the y axis, and H_x is the angular momentum of the in-cylinder gas about the x axis. M_y is the moment of inertia about the y axis, and M_x is the moment of inertia about the

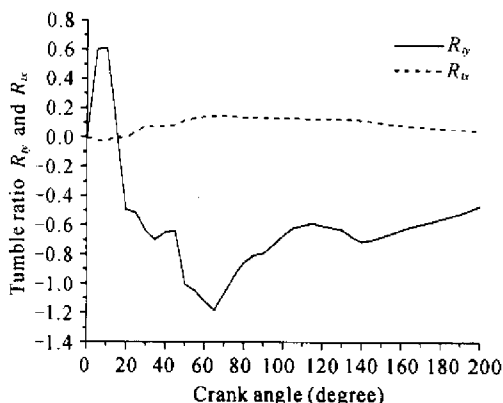


Fig. 7 Variation of tumble ratios R_{ty} and R_{tx} vs crank angle

4. Result validation

Laser diagnostic measurements of the in-

x axis. ω is the crankshaft rotation speed (r/min).

Fig. 7 shows variations in the R_{ty} and R_{tx} with respect to the crank angle. During the backflow phase, the in-cylinder gas rotation is anti-clockwise ($R_{ty} > 0$) in general. During the intake flow phase, the rotation is clockwise ($R_{ty} < 0$). Tumble ratio R_{ty} is initially increased by the strong intake flow and reaches a maximum at about 65° CA. Then it decreases due to a weak intake flow and downward motion of the piston until the intake valve closure. The downward piston motion increases the moment of inertia about the y -axis, resulting in a decrease in R_{ty} . From 120° CA to 140° CA, R_{ty} increases a little. Tumble ratio R_{tx} is approximately zero owing to the symmetric geometry about the xz -plane.

In-cylinder mean pressure p_{cyl} is an important parameter for the in-cylinder gas state. Fig. 8 shows the variation in p_{cyl} with respect to the crank angle. It indicates that the in-cylinder mean pressure fluctuates during the intake process. Shortly after the intake valve opening, the in-cylinder mean pressure decreases rapidly from 115 kPa to 65 kPa in 20 degrees of crank angle. It is caused by the backflow and the downward piston motion. p_{cyl} reaches a maximum 88 kPa at about 100° CA, which is over the intake pressure 85 kPa. At intake valve closure, the in-cylinder mean pressure is 78.5 kPa, lower than the intake pressure by 7.6%.

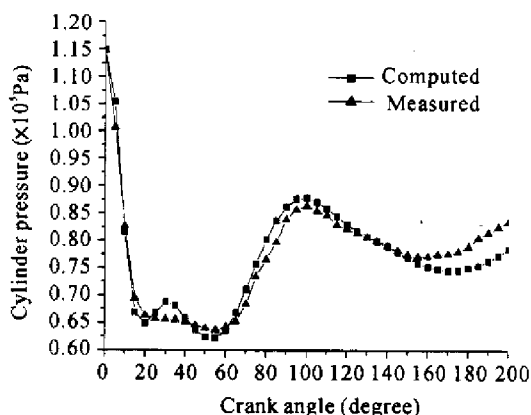


Fig. 8 Comparison of computed and measured cylinder pressure

cylinder flow field by laser doppler velocimetry (LDV) or the particle image velocimetry (PIV) are widely used to validate the three-dimensional

simulation results (Kim *et al.*, 2000; Jones *et al.*, 1995). However, they are limited by the optical accesses and the signal sampling. At present, it is difficult to perform velocity measurements for the transient flow fields in high-speed small engines with bores under 60 mm and speeds over 3000 r/min. In this paper, the cylinder pressure is measured on the running engine to validate the calculated results.

Because of the comparatively low cylinder pressure during the intake process, the type SYC-03B low-pressure piezoelectric transducer with high sensitivity is adopted to measure the cylinder pressure. The type CB466 combustion analyzing system is used to collect data and observe online. Fig. 8 shows cylinder pressures versus crank angle for the experiment and computation during the intake process and shows that they agreed well. During the late intake process, the computational pressure is lower than the measured pressure and the maximum difference is about 6%. This could be due to the absence of intake-exhaust valve overlaps. In addition, the boundary condition at the intake port inlet is assumed to be a constant pressure in calculation, while the pressure at the port inlet is actually variable. This discrepancy can also cause errors.

CONCLUSIONS

The newly developed body-fitted valve three-dimensional analytical model for transient intake flow put forward in this paper can be used to treat vertical and inclined valves. The analytical model was used for numerical simulation of the 3D transient flow in the intake process of a two-valve engine with a semi-sphere combustion chamber and a radial intake port. Detailed information on the flow field was obtained. Simulation results are helpful for gaining understanding of the complex flow phenomena during the intake process, and provide theoretical basis for optimizing the structure of the engine intake system.

References

- Amsden, A. A., O'Rourke, P. J. and Butler, T. D., 1989. KIVA-II: A computer program for chemically reactive flows with sprays. Los Alamos National Laboratory Report LA-11560-MS.
- Amsden, A. A., 1993. KIVA-3: A KIVA program with block-structured mesh for complex geometries. Los Alamos National Laboratory Report LA-12503-MS.
- Hessel, R.P., 1993. Numerical simulation of valved intake port and in-cylinder flows using KIVA 3. PhD Thesis, University of Wisconsin, US.
- Hirt, C.W., Amsden, A.A. and Cook, J.L., 1974. An arbitrary Lagrangian-Eulerian computing method for all flow speeds. *J. Comp. Phys.*, **14**: 227-243.
- Iwamoto, K., Noma, K., Nakayama, O., Yamauchi, Y. and Ando, H., 1997. Development of gasoline direct injection engine. *SAE 970541*.
- Jones, P. and Junday, J.S., 1995. Full cycle computational fluid dynamics calculations in a motored valve pent roof combustion chamber and comparison with experiment. *SAE 950286*.
- Kaoru, Horie., Nishizawa, K., Ogawa, T., Akuzaki, S. and Miura, K., 1992. The development of a high fuel economy and high performance four-valved lean burn engine. *SAE 920455*.
- Kim, W.T., Huh, K.Y., Lee, J.W. and Kang, K.Y., 2000. Numerical simulation of intake and compression flow in a four-valve pent-roof spark ignition engine and validation with LDV data. *Proc Instn Mech Engrs*, **214** (Part D): 361 – 372.
- Luo, M.J., Ye, X.M., Chen, G.H. and Jiang, Y.K., 2000. Three-dimensional block-structured body-fitted grid generation in intake manifolds of internal combustion engines. *Journal of Huazhong University of Science And Technology*, **28**(12): 70 – 72(in Chinese).
- Luo, M.J., Chen, G.H., Ma, Y.H. and Ye, X.M., 2001. Study on Three-dimensional Flow Modeling of Multi-cylinder Vehicle Engine Inlet Manifold and its Application. Proceeding of the Eleventh International Pacific Conference on Automotive Engineering (in Chinese).
- Reeves, M., Towers, D.P., Tavender, B. and Buckbeny, C.H., 1999. A high-speed all-digital technique for cycle-resolved 2-D flow measurement and flow visualization within SI engine cylinders. *Optics and Lasers Engineering*, **31**: 247 – 261.
- Reuss, D.L., Adrian, R.J., Landreth, C.C., French, D.T. and Fansler, T.D., 1989. Instantaneous planar measurements of velocity and large scale vorticity and strain rate in an engine using particle-image velocimetry. *SAE 890616*.
- Shi, S.X., 2001. Recent progress in combustion technologies for automotive engines. *Combustion Science and Technology*, **7**(1): 1 – 15(in Chinese).